

## GRAIL TCM-5 GO/NO-GO: DEVELOPING LUNAR ORBIT INSERTION CRITERIA

Min-Kun J. Chung,<sup>\*</sup>

The Gravity Recovery and Interior Laboratory (GRAIL) mission successfully completed mapping the Moon's gravity field to an unprecedented level. The mission success was critically dependent on the success of the Lunar Orbit Insertion (LOI). It was somewhat unfamiliar as it involved an elliptical approach from a low-energy trans-lunar cruise trajectory via Sun-Earth three-body region rather than a more conventional hyperbolic approach from a direct Earth-to-Moon transfer. In addition, how its delivery dispersion affected the science formation of the two spacecraft was not well understood. In this paper we establish a set of LOI criteria to meet all the requirements and we use these criteria to establish Go/No-Go boundaries of the last, statistical Trajectory Correction Maneuvers (TCM-5s) for operations. In the end both spacecraft were found to be within the established boundaries and TCM-5s of both spacecraft were cancelled.

### INTRODUCTION

Two Gravity Recovery and Interior Laboratory (GRAIL) spacecraft were launched on a Delta II 7920H 10C launch vehicle on 10-Sep-2011 to map the lunar gravity field to unprecedented accuracy and resolution in order to better understand the internal structure and thermal evolution of the Moon. Refer to Reference 1 for the details of the mission overview.<sup>1</sup> The GRAIL mission used a three-month long, high-thrust, low-energy Trans-Lunar Cruise (TLC) trajectory over a short, direct transfer to the Moon for some operational advantages and Lunar Orbit Insertion (LOI) delta-v ( $\Delta V$ ) savings. It had a launch energy higher than that of the more conventional direct transfer to the Moon but lower LOI  $\Delta V$ . Refer to Reference 2 for more details on the TLC trajectory.<sup>2</sup> The LOI captured the spacecraft into an 11.5-hour orbit around the Moon. Before the Science Phase could begin, the orbit periods had to be reduced and the two spacecraft had to be placed in a science formation via a series of orbital maneuvers. Refer to Reference 3 for more details on these orbital maneuvers.<sup>3</sup>

After an accurate injection, the first Trajectory Correction Maneuvers (TCM-1) were canceled on both spacecraft since the two following deterministic TCMs (TCM-2 and TCM-3) could be re-optimized to target the Lunar Orbit Insertion (LOI) targets precisely with no additional  $\Delta V$ .<sup>†</sup> In the original TLC reference trajectories, TCM-2 and TCM-3 were the only deterministic TCMs to separate the two LOIs by one day and to insert into the manifolds that led to LOI. However, in

---

<sup>\*</sup> Mission Design Engineer, Jet Propulsion Laboratory, California Institute of Technology, M/S 301-121, 4800 Oak Grove Drive, Pasadena, CA 91109.

<sup>†</sup> Maneuver names are abbreviated with a spacecraft letter and a maneuver number. For example, "TCM-A1" stands for TCM number 1 on GR-A spacecraft. Also, "TCM-1" refers to both TCM-A1 and TCM-B1.

operations the project decided to design the LOI maneuver prior to the TCM-3 execution. This decision forced TCM-4 to be a deterministic maneuver targeting the full 6-state LOI targets along with TCM-3. Thus, TCM-5 (8 days before LOI) became the only statistical maneuver correcting the maneuver execution errors stemming from TCM-3 and TCM-4.

Refer to Figure 1 below for the TLC trajectories from launch to LOI as well as the placement of TCMs. The dotted line represents the trajectory below the plain of the paper while the solid represents that above the plain of the paper. The red is for GRAIL-A (GR-A) whereas the blue is for GRAIL-B (GR-B).

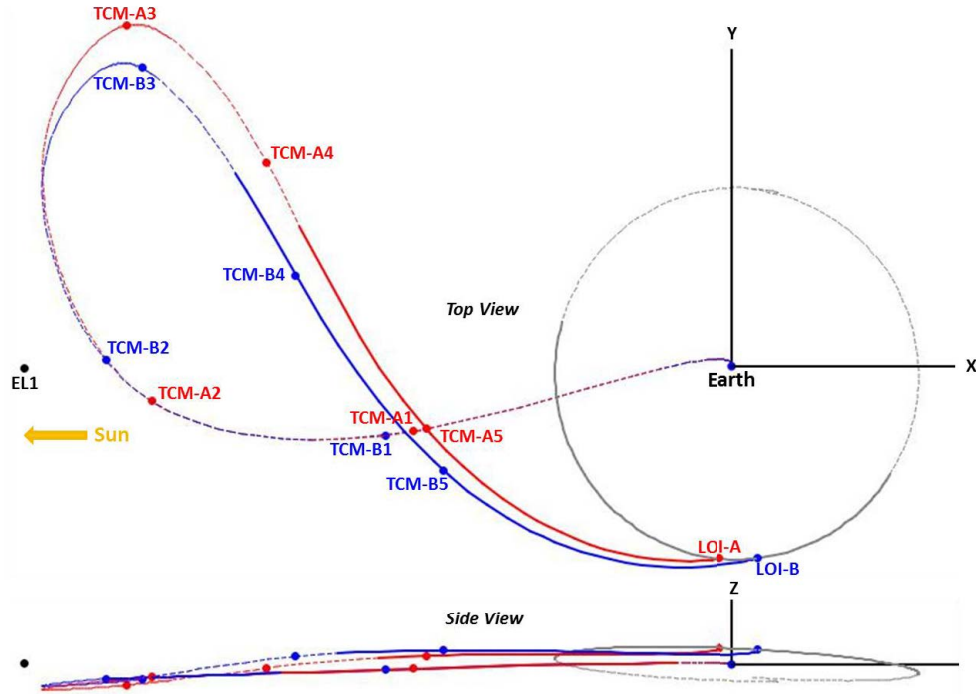


**Figure 1. GRAIL TLC Trajectories in Earth-centered, Sun-Earth Rotating Frame.**

The GRAIL navigation team was well aware of the importance of establishing a set of criteria for LOI: first, to ascertain that there exists a space in the LOI delivery wide enough for a successful Science Phase when corrected by TCM-5; second, to determine whether TCM-5 was required or not. JPL Mission Design and Navigation Section software, Linear Analysis of Maneuvers with Bounds and Inequality Constraints (LAMBIC), was used for the statistical maneuver analyses of the TLC trajectory.<sup>4</sup> However, this linear tool could not be used effectively for the non-linear dynamics involved in the low lunar orbits. An alternate, simpler approach was sought for as the time of TCM-5 was approaching fast.

## PRELIMINARY CONSIDERATIONS

As a product of the LAMBIC analyses, LOI delivery statistics from TCM-4 and TCM-5 were obtained in terms of the dispersion sigma on each of the six LOI delivery parameters: semi-major axis (SMA), periapsis range or radius at closest approach (RCA), Inclination (INC), longitude of ascending node (LAN), argument of periapsis (AOP), and time to periapsis (TTP). Refer to Table

1 below for the LOI delivery dispersion sigma values with respect to TCM-4 and TCM-5 for both spacecraft (the angles are in EME2000).

**Table 1. LOI Delivery Dispersions from TCM-4 and TCM-5.\***

| LOI delivery Parameters | TCM-4 ( $3\sigma$ ) |       | TCM-5 ( $3\sigma$ ) |       |
|-------------------------|---------------------|-------|---------------------|-------|
|                         | GR-A                | GR-B  | GR-A                | GR-B  |
| SMA (km)                | 293.9               | 800.7 | 286.3               | 791.6 |
| RCA (km)                | 2.590               | 1.929 | 1.091               | 1.060 |
| INC (deg)               | 0.095               | 0.091 | 0.028               | 0.032 |
| LAN (deg)               | 0.048               | 0.060 | 0.041               | 0.058 |
| AOP (deg)               | 0.074               | 0.074 | 0.072               | 0.074 |
| TTP (sec)               | 170.5               | 112.6 | 27.5                | 26.5  |

First, to ensure all the science requirements can be met with the execution of TCM-5, we must show that the LOI delivery dispersions of  $\pm 3$  sigma ( $\pm 3\sigma$ ) TCM-5 values can be handled adequately by the subsequent orbital maneuvers leading up to the Science Phase. Second, to be able to cancel TCM-5, we need to show that  $\pm 3\sigma$  TCM-4 dispersions can be handled adequately. Or, if some  $\pm 3\sigma$  TCM-4 dispersions are too large to be handled adequately, some boundaries on those parameters need to be established such that the dispersion within the boundary can be handled adequately by the subsequent orbital maneuvers.

In a typical hyperbolic approach, the problem usually reduces to two simple targets,  $\mathbf{B}\cdot\mathbf{R}$  and  $\mathbf{B}\cdot\mathbf{T}$ ,<sup>†</sup> while minimizing  $\Delta V$ . However, since GRAIL LOI was an elliptical approach from a low-energy TLC trajectory and the objective was not only to minimize  $\Delta V$  but also more importantly to place the two spacecraft in the science formation, it was not so apparent which of the LOI delivery parameters were more critical.

### Derived Requirements during Orbital Phases

Before we proceed any further, it is necessary to review the derived requirements in the orbital phases leading up to the Science Phase that meets all the science requirements. There are three GRAIL-defined orbital phases before the Science Phase: LOI Phase, Orbit Period Reduction (OPR) Phase, and Transition to Science Formation (TSF) Phase. The orbital maneuvers are designed such that the orbits of GR-A and GR-B do not cross nor come closer than 10 km: Collision Avoidance (COLA). In this sub-section we identify what the derived requirements are in each of the three orbital phases.

*LOI Phase.* The objective of the LOI Phase is to capture the spacecraft into an 11.5-hour orbit. LOI-A is about 25 hours ahead of LOI-B primarily for operational simplicity but also for COLA.

---

\* This LAMBIC analysis on the TLC trajectory was performed by Ram Bhat (Maneuver Analyst, JPL) based on the post-TCM-3 orbit determination solution number 17, version 1 (od017v1).

<sup>†</sup> In a hyperbolic approach, the flyby miss vector  $\mathbf{B}$  is a vector from the center body to the point where the incoming v-infinity vector direction  $\mathbf{S}$  of the spacecraft penetrates the plane normal to  $\mathbf{S}$ .  $\mathbf{B}\cdot\mathbf{T}$  is the component along the  $\mathbf{T}$ , which is normal to  $\mathbf{S}$  and parallel to the Earth Mean Equator and Equinox of 2000 (EME2000).  $\mathbf{B}\cdot\mathbf{R}$  is the component along  $\mathbf{R} = \mathbf{S} \times \mathbf{T}$ .

*OPR Phase.* The maneuvers in the OPR Phase are named Period Reduction Maneuvers (PRMs). There are two clusters of PRMs for each spacecraft. The first cluster has three maneuvers (PRM-1 through 3) and the second has four (PRM-4 through 7). The maneuvers in each cluster are executed with only one maneuver design for operational simplicity. The first one is designed normally and the subsequent ones within the same cluster are simply repositioned around the periapsis. PRM-A1 through 3 occur one week ahead of PRM-B1 through 3. After about a week and a half later, PRM-A4 through 7 occur one week ahead of PRM-B4 through 7. The objective of the OPR Phase is to reduce the orbit periods nearly to the science orbit period without violating COLA: the first cluster targets 3.65 and 3.85 hour for GR-A and GR-B, respectively; the second cluster targets 1.904 and 1.950 hour for GR-A and GR-B, respectively.

*TSF Phase.* The objective of the TSF Phase is to reduce the orbit periods slowly without violating COLA to the science orbit period, to remove any remaining out-of-plane component (inclination and node), to keep the maneuvers reasonably small, and to set the final eccentricity ( $e$ ) and the argument of periapsis ( $\omega$ ) in the farthest position in the  $e$ - $\omega$  space from the  $e$ - $\omega$  evolution of the science orbits to avoid any periapsis-raising maneuver during the whole Science Phase (3 months). The maneuvers in the TSF Phase are named Transition to Science formation phase Maneuvers (TSMs): TSM-A1, TSM-B1, TSM-A2, TSM-B2, and TSM-B3 in the order of execution.

Incidentally, the  $e$ - $\omega$  evolution is best visualized in an  $e$ - $\omega$  plot, where  $e$  is the radius and  $\omega$  is the angle in a polar plot. One can visualize the plot as the movement of a perilune, where the angle is the argument of latitude for a polar orbit. The orbit is circular at the center (zero  $e$ ), and it becomes more eccentric away from the center. Also, the maneuver magnitude can be estimated from the line length and direction of a maneuver in the  $e$ - $\omega$  plot. Refer to Reference 5 for more details on  $e$ - $\omega$  space.<sup>5</sup> Figure 2 below shows the  $e$ - $\omega$  plot of the GRAIL reference orbit in the TSF Phase. The green  $e$  arc represents a 15 km spherical altitude and the red  $e$  arc represents 10 km. Both altitudes are estimated from a 1.9-hour orbit (since it corresponds to a post TSM-A1 and TSM-B1). In general, the  $e$ - $\omega$  evolution in the TSF Phase starts from the top-right corner and ends at the bottom-left corner. The end point corresponds to the beginning of the Science Phase, where the two spacecraft are placed in the required science formation. The direction of each maneuver (indicated by a letter and a number but without the maneuver name “TSM-”) is from “-” to “+.”

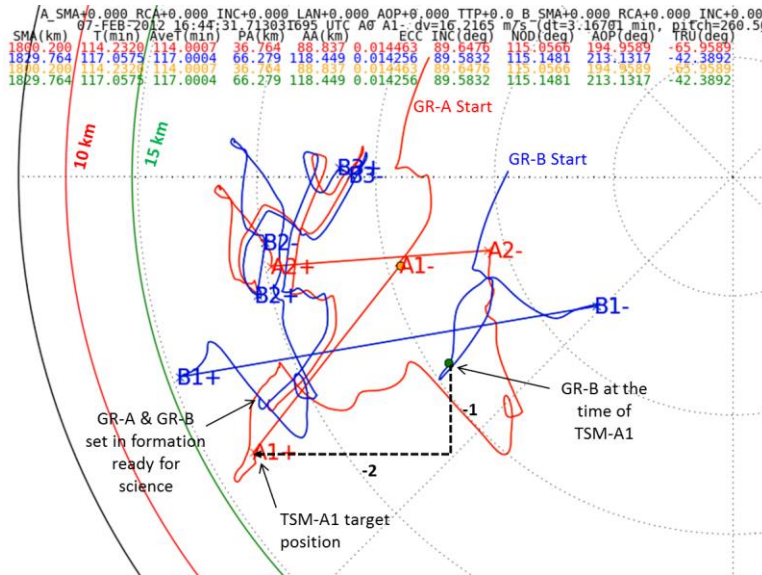


**Figure 2.  $e$ - $\omega$  Plot during the TSF Phase.**

TSM-A1 reduces the period to 1.9 hour, while targeting an  $e-\omega$  position along the line with a slope of  $-1/2$  or  $(\Delta x, \Delta y) = (-2, -1)$  from the GR-B  $e-\omega$  position at the time of TSM-A1. Refer to Figure 2 above. The period difference between GR-A and GR-B (3 minutes) after TSM-A1 allows GR-A to lap GR-B in orbit once in 3 days. The maximum TSM-A1 magnitude is 25 m/s.

TSM-B1 reduces the period to 1.9 hour (the same as GR-A) when GR-B is  $\sim 27.8$  minutes ahead of GR-A. The maximum TSM-B1 is 30 m/s. Also, the TSM-B1  $e-\omega$  target should be set such that its  $e-\omega$  evolution along with TSM-B2 eventually leads to a small TSM-B3 magnitude.

TSM-A2 sets the period to that of the science orbit (1.8919 hour). The TSM-A2  $e-\omega$  target is such that it moves to a farthest location (with an acceptable minimum topographic altitude  $> 10$  km) in the  $e-\omega$  evolution such that there is no need for a periapsis-raising maneuver for the entire Science Phase (3 months). This target position usually is near the left-bottom corner of the  $e-\omega$  plot. The maximum TSM-A2 magnitude is 25 m/s.

TSM-B2 reduces the period slightly higher than that of GR-A (1.8935 hour) to manage the separation in the event of execution error. TSM-B2 also removes any out-of-plane component (inclination and node). After TSM-B2, GR-A and GR-B positions in  $e-\omega$  plot should be close. The maximum TSM-B2 magnitude is 25 m/s.

TSM-B3 reduces the period just slightly below (29 sec) the science orbit period for a desired separation range rate (initially positive). The maximum TSM-B3 magnitude is 5 m/s to reduce the execution error for the science formation.\*

The maximum  $\Delta V$  of each maneuver of TSMs was derived such that the propagation of the execution error does not exceed the expected limit for a successful science formation at the end of the TSF Phase.

### Initial Pilot Runs<sup>†</sup>

As already mentioned above, in the absence of a non-linear statistical maneuver analysis tool one may have tried, for example, a 1,000-sample Monte Carlo analysis. However, it was ruled out for each case taking too long and for some cases requiring human attention.<sup>‡</sup>

Since it was not still well understood how LOIs, PRMs, and especially TSMs would respond under the LOI delivery dispersion, and since we wanted to reduce the number of runs, the following two sets of runs were made initially: (1) TCM-5  $\pm 3\sigma$  combination set and (2) TCM-4  $\pm 3\sigma$  combination set. For each LOI delivery parameter either a  $+3\sigma$  or  $-3\sigma$  value was assigned to construct a GR-A dispersion case. And for every GR-A case thus constructed, a GR-B dispersion

---

\* Unfortunately the algorithm to minimize TSM-B3  $\Delta V$  magnitude was not robustly implemented; it yielded  $\Delta V$  higher than 5 m/s for some cases. A sophisticated algorithm could have also used TSM-A2 target to keep the TSM-B3 magnitude small.

<sup>†</sup> Credit goes to Sara Hatch (Trajectory Analysis, JPL) for implementing the scripts for the nominal reference orbits. These initial pilot runs were using these scripts; however, when  $\pm 3\sigma$  LOI delivery dispersions were introduced, they had to be updated for the cases involving  $\pm 3\sigma$  LOI delivery dispersions, especially for TSM-A1 and TSM-B1 optimizations. Unfortunately, there was not enough time to update them completely; there were still some cases that had to be resolved by hand, such as those involving TSM-B3  $\Delta V$  magnitude exceeding 5 m/s.

<sup>‡</sup> First, each case took on the order of several hours to propagate the orbits through the orbital maneuvers from LOI Phase to TSF Phase and to optimize maneuvers from LOIs to TSMs. Second, the maneuver optimization scripts use an optimization interface script that computes the partials by a finite differencing; thus, it takes long not only due to calling the cost and constraint functions multiple times but also due to the lower precision of the finite differencing partials. Depending on where the optimizer quits, a maneuver optimization could yield an unexpected result; such cases had to be resolved by hand.

case was constructed by assigning an opposite  $3\sigma$  value from GR-A for each LOI delivery parameter. For example, GR-A( $+3\sigma, -3\sigma, +3\sigma, -3\sigma, +3\sigma, +3\sigma$ ) is combined with GR-B( $-3\sigma, +3\sigma, -3\sigma, +3\sigma, -3\sigma, -3\sigma$ ) to compose one case, assuming the parameter ordering as (SMA, RCA, INC, NOD, AOP, TTP). Each set thus constructed has 64 cases. The first set with TCM-5  $\pm 3\sigma$  values was motivated by the fact that, if the majority of the first set cases succeed, then we would be confident that the execution of TCM-5 would make the mission. Similarly, the second set with TCM-4  $\pm 3\sigma$  values were motivated by the fact that, if the majority of the second set cases succeed, we would be confident that the execution of TCM-5 may be skipped.

*TCM-5  $\pm 3\sigma$  Combination Result.* All 64 cases completed. Two of them were finished by hand. Seven of the runs had TSM-B5 over 5 m/s, but they are probably correctable by hand as at least one case with TSM-B3 over 5 m/s could be corrected. So, initially we felt somewhat confident that with the execution of TCM-5 we could make the mission.

*TCM-4  $\pm 3\sigma$  Combination Result.* However, the second set of initial runs were more challenging. Five cases did not complete or took longer than 24 hours, mostly having difficulty with TSM-B1 optimization. Nine cases had TSM-B1 over 30 m/s. Five cases had TSM-B3 over 5 m/s. One particular case that had TSM-B1, TSM-B2, and TSM-B3 magnitude of 33 m/s, 6.9 m/s, and 8.5 m/s, respectively could be corrected to 28.3 m/s, 7.0 m/s, and 0.7 m/s by hand, however.\*

Therefore, from the result of these pilot runs, we felt confident that with the execution of TCM-5 we would be able to make the mission, while we suspected that there would be some challenging cases where we would not be able to cancel TCM-5.

Next we examined the effect of the LOI delivery dispersion on each parameter individually to understand whether there is any particular parameter more critical than others.

### **Examining Each GR-A LOI Delivery Dispersion Individually**

In this sub-section the behavior of  $\pm 3\sigma$  TCM-A4 LOI delivery dispersion of each parameter is examined against the nominal GR-B. For example, the first case in SMA is GR-A( $\pm 3\sigma, 0, 0, 0, 0, 0$ ) + GR-B(0, 0, 0, 0, 0, 0), and the second case in RCA is GR-A(0,  $\pm 3\sigma, 0, 0, 0, 0$ ) + GR-B(0, 0, 0, 0, 0, 0), etc.† Each figure below shows via an  $e$ - $\omega$  plot the result of what TSMS did to set the two spacecraft in the required science formation, where GR-A begins with  $\pm 3\sigma$  dispersion of the specified parameter and GR-B begins nominally at LOI. The color scheme in the plots is as follows: orange and green for the nominal GR-A and B, respectively; red and blue for the dispersed GR-A and B, respectively.

---

\* As stated before, these initial results were using the original scripts before updates.

† The same notation (SMA, RCA, INC, NOD, AOP, TTP) applies here as before.

*Dispersion in SMA.* Figure 3 below shows the result of what the TSMs did to set the two spacecraft in the required science formation when GR-A begins with  $\pm 3\sigma$  SMA dispersion (and nominally in other parameters) and GR-B begins nominally at LOI. The left plot shows the  $-3\sigma$  case whereas the right one shows the  $+3\sigma$  case. It appears that the SMA dispersions at LOI are well handled by LOIs and PRMs so that they have very little effect on the  $e$ - $\omega$  space when the TSF Phase begins. As result, the TSMs do almost the same jobs in this dispersed case as they do in the nominal case, especially the  $+3\sigma$  case.

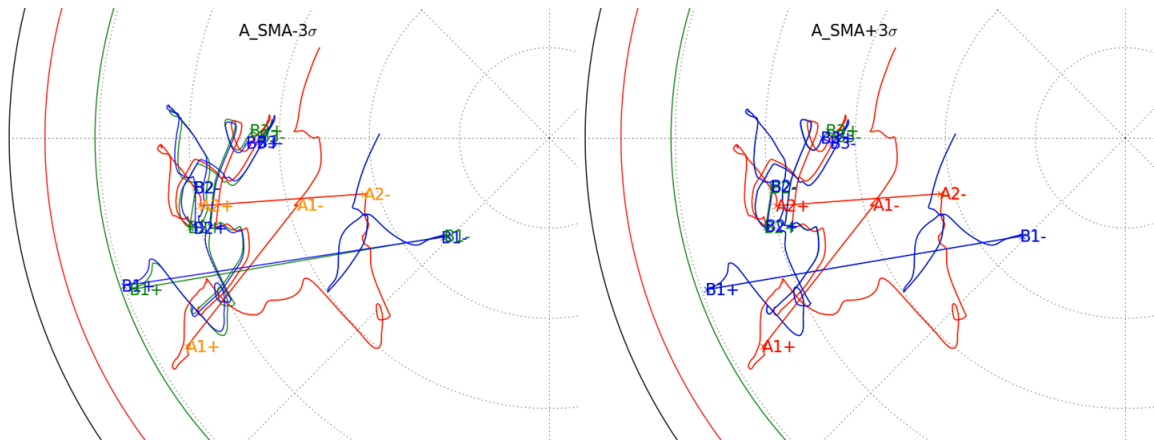


**Figure 3. GR-A  $\pm 3\sigma$  SMA Dispersion.**

*Dispersion in RCA.* From Figure 4 below, the effect of  $\pm 3\sigma$  RCA dispersion on GR-A is more pronounced at the start of the TSF Phase (note the separation of the red dispersed case from the orange nominal case); however, TSM-A1 effectively handles it, placing GR-A close to the nominal position in the  $e$ - $\omega$  space.

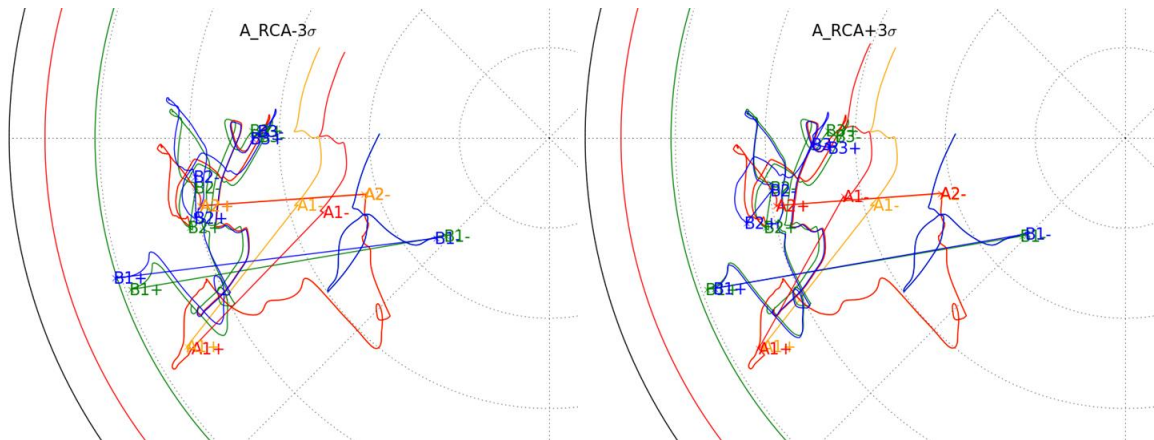


**Figure 4. GR-A  $\pm 3\sigma$  RCA Dispersion.**

*Dispersion in INC.* From Figure 5 below,  $\pm 3\sigma$  INC dispersion is noticeable but small. Its small effect is not handled by TSM-A1 completely (note that the small separation between the red dispersed case and the orange nominal case remains at TSM-A2). However, TSM-A2 removes most of the separation, and TSM-B2 removes the inclination difference effectively by changing GR-B inclination to that of GR-A.

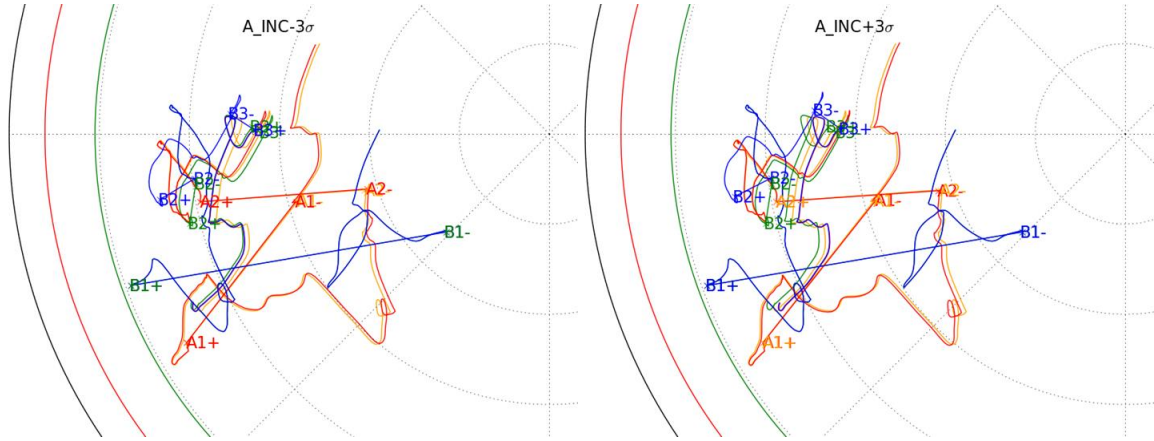


**Figure 5. GR-A  $\pm 3\sigma$  INC Dispersion.**

*Dispersion in LAN.* From Figure 6 below,  $\pm 3\sigma$  LAN dispersion on GR-A is hardly noticeable from the nominal in the  $e$ - $\omega$  space at the start of the TSF Phase. TSM-B2 effectively handles the small out-of-plane difference.

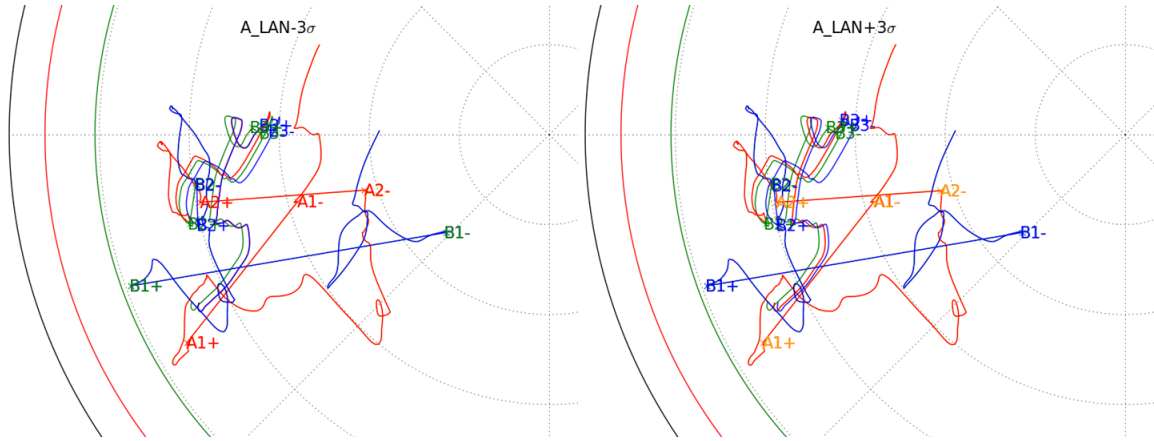


**Figure 6. GR-A  $\pm 3\sigma$  LAN Dispersion.**

*Dispersion in AOP.* From Figure 7 below,  $\pm 3\sigma$  AOP dispersion on GR-A is noticeable but small. TSM-A1 effectively handles the difference, leaving the rest of the TSF Phase to appear similar to the nominal case, especially for the  $-3\sigma$  case.

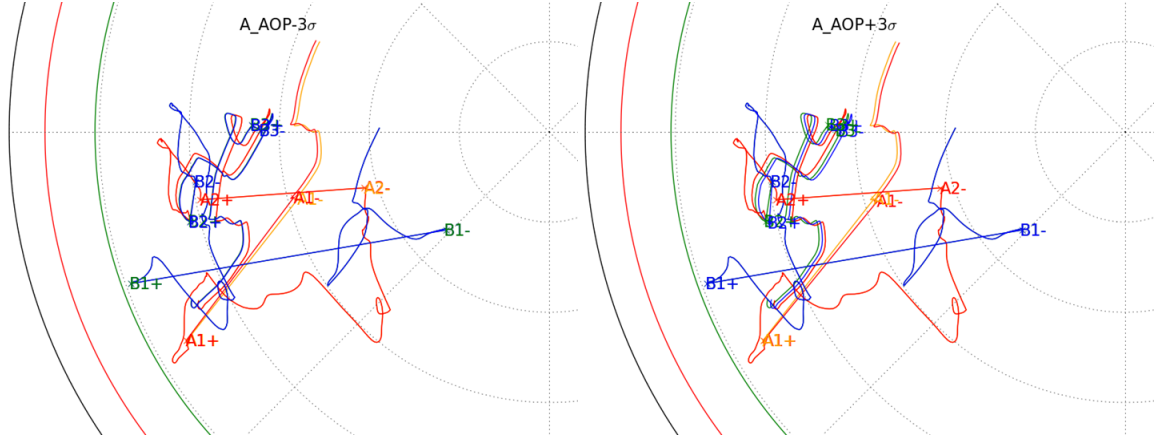


**Figure 7. GR-A  $\pm 3\sigma$  AOP Dispersion.**

*Dispersion in TTP.* From Figure 8 below,  $\pm 3\sigma$  TTP dispersion on GR-A is quite distinct in the beginning of TSF Phase. However, TSM-A1 reduced the difference considerably in the  $e$ - $\omega$  space, and TSM-A2 further removes it almost completely. Also, although not shown in the plot, the  $+3\sigma$  case violates 10-km OPR COLA requirement ( $\sim 4$  km). The OPR COLA requirement will be examined more carefully in a later section.

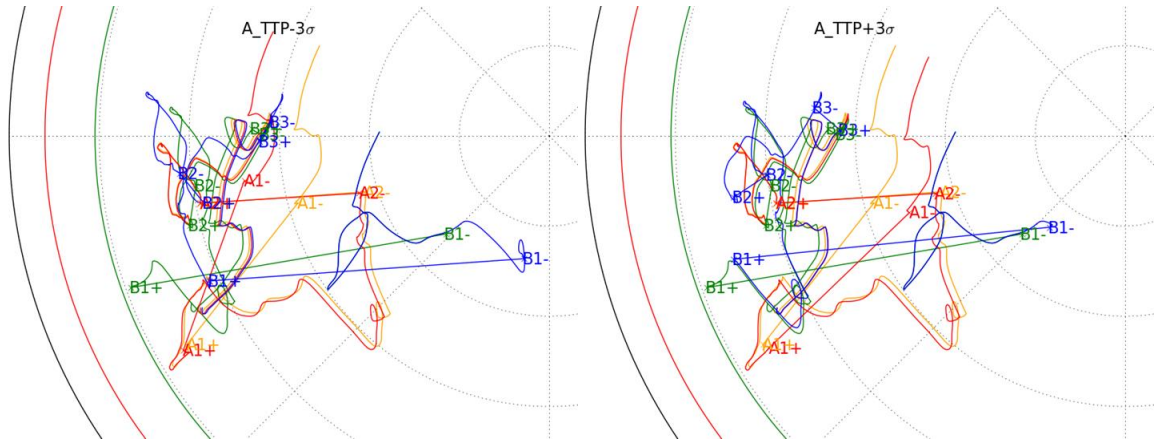


**Figure 8. GR-A  $\pm 3\sigma$  TTP Dispersion.**

Examining each of the 12 cases above against the TSF derived requirements, we found only one item that was violated: OPR COLA ( $\sim 4$  km  $<$  10 km) for the  $-3\sigma$  TTP dispersion case.

Thus, we conclude that any  $\pm 3\sigma$  LOI delivery dispersions from TCM-A4 are handled effectively by the TSMs as long as GR-B dispersions remain near the nominal. Before pursuing the combined effect of GR-A dispersions as well as the GR-B dispersion being greater than the nominal, we examine the effect of individual GR-B dispersions first.

### Examining Each GR-B LOI Delivery Dispersion Individually

As we examined the effect of GR-A  $\pm 3\sigma$  dispersions above, in this sub-section we focus on the behavior of  $\pm 3\sigma$  LOI delivery dispersion of each GR-B parameter against the nominal GR-A by examining the evolution in the  $e-\omega$  plots.

*Dispersion in SMA.* Figure 9 below shows the effect of  $\pm 3\sigma$  SMA dispersion on GR-B, which is barely noticeable in the beginning of the TSF Phase. The dispersion is well taken care of by TSMs to set the formation for science.

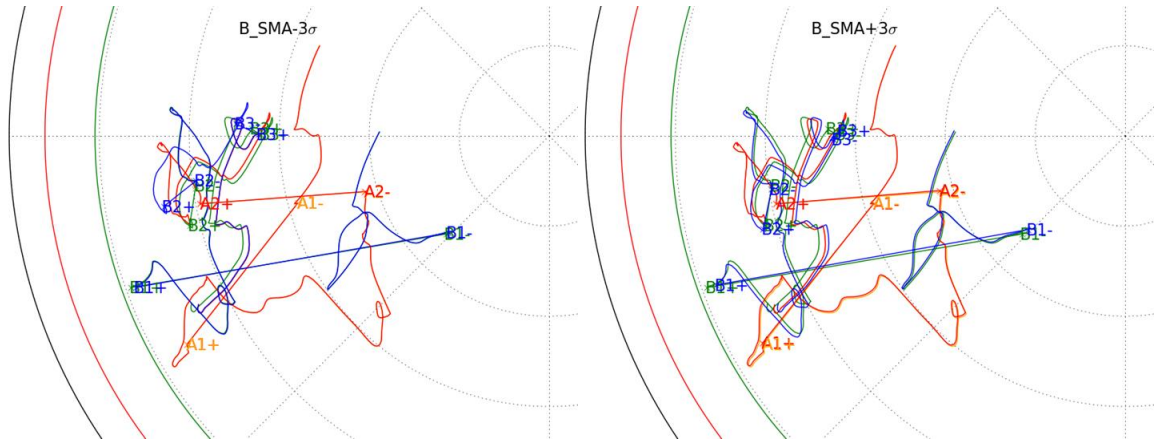


**Figure 9. GR-B  $\pm 3\sigma$  SMA Dispersion.**

*Dispersion in RCA.* From Figure 10 below,  $\pm 3\sigma$  RCA dispersion on GR-B is more noticeable in the beginning of the TSF Phase. Note TSM-A1's tendency to match GR-B in the  $e-\omega$  space so as to make the magnitude of TSM-A2 more reasonable (note that the length and direction of a maneuver in the  $e-\omega$  space is related to the  $\Delta V$  magnitude).

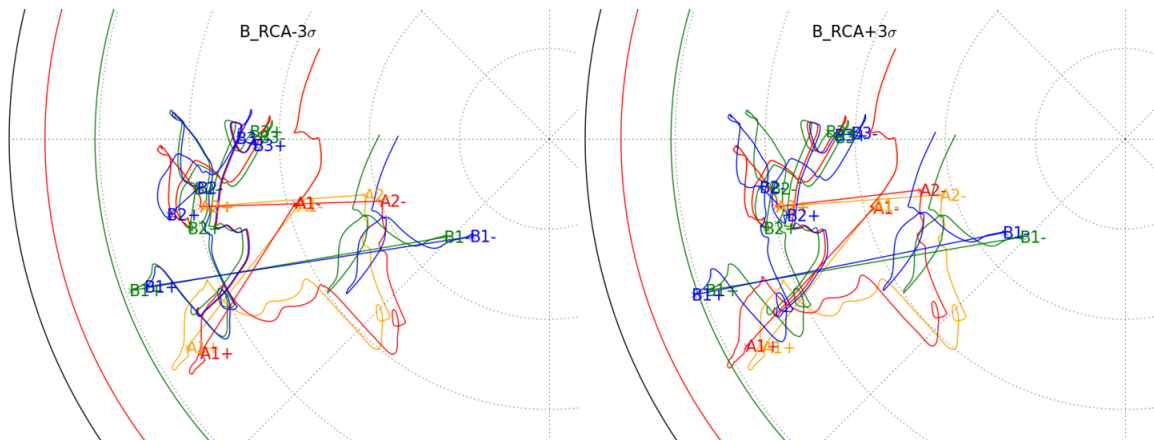


**Figure 10. GR-B  $\pm 3\sigma$  RCA Dispersion.**

*Dispersion in INC.* From Figure 11 below,  $\pm 3\sigma$  INC dispersion on GR-B is hardly noticeable in the beginning of the TSF Phase. TSM-B2 effectively matches GR-B's inclination to that of GR-A.

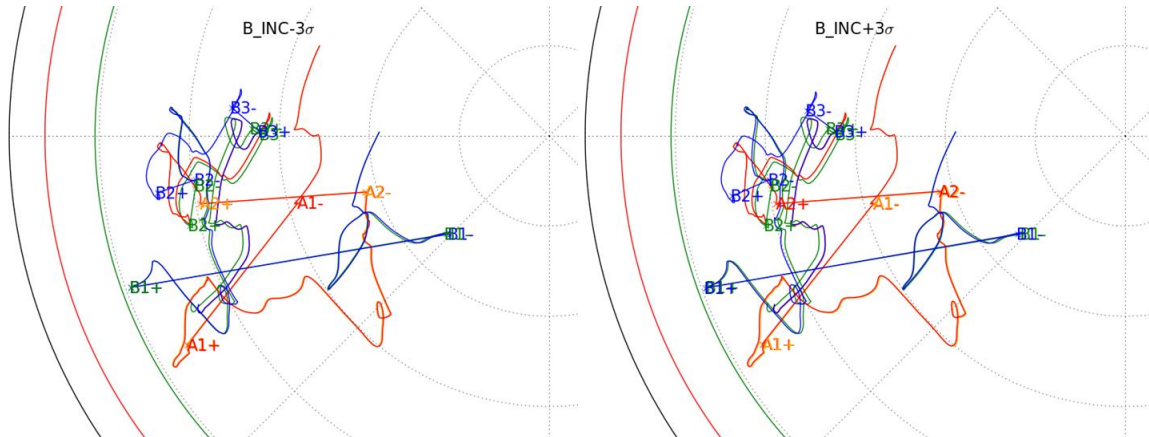


**Figure 11. GR-B  $\pm 3\sigma$  INC Dispersion.**

*Dispersion in LAN.* Similarly from Figure 12 below,  $\pm 3\sigma$  LAN dispersion on GR-B is even less noticeable in the beginning of the TSF Phase. TSM-B2 effectively matches GR-B's node to that of GR-A.

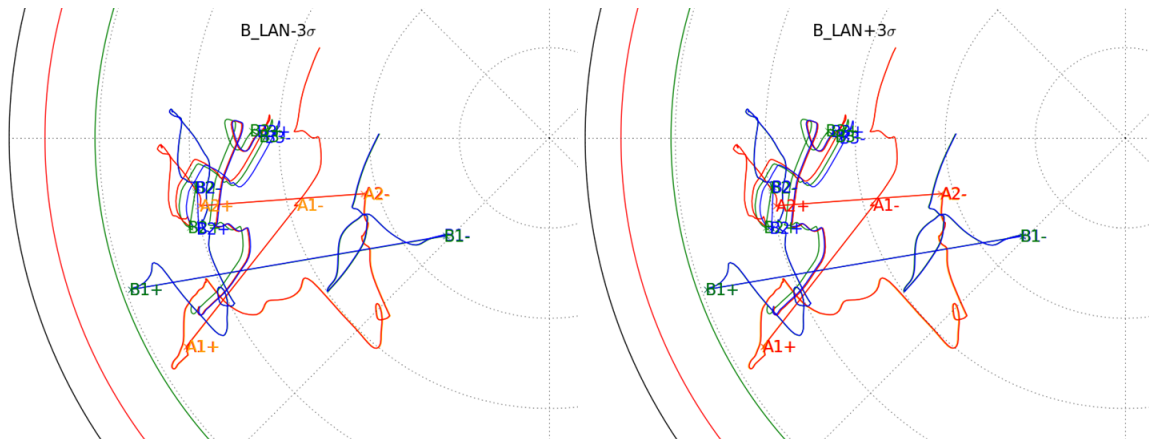


**Figure 12. GR-B  $\pm 3\sigma$  LAN Dispersion.**

*Dispersion in AOP.* From Figure 13 below,  $\pm 3\sigma$  AOP dispersion on GR-B is small but noticeable in the beginning of the TSF Phase. Note again TSM-A1's tendency to match GR-B in the  $e-\omega$  space. Since this case is different from the nominal solely in AOP, the dispersed case is literally shifted in the  $e-\omega$  space and even the direction of TSM-B2, which removes the out-of-plane component, remains quite the same.

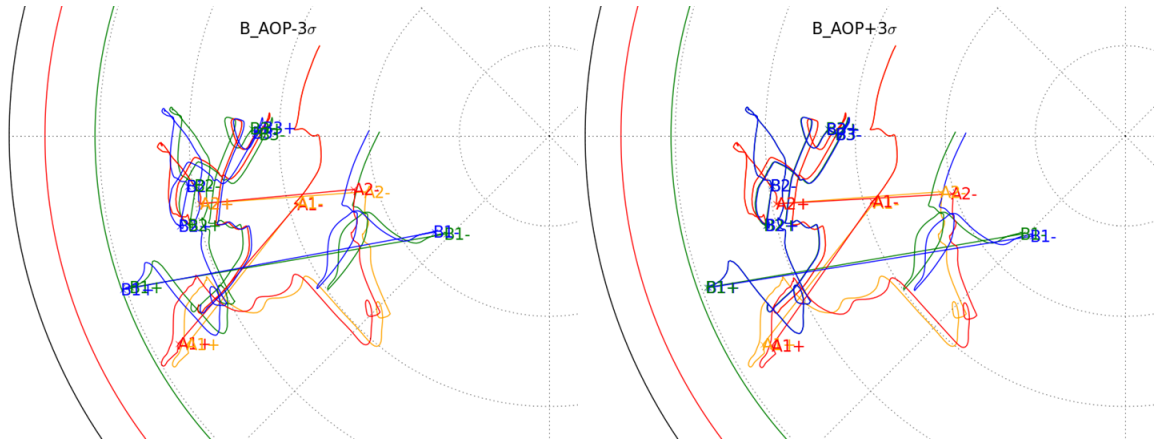


**Figure 13. GR-B  $\pm 3\sigma$  AOP Dispersion.**

*Dispersion in TTP.* From Figure 14 below,  $\pm 3\sigma$  TTP dispersion on GR-B is most noticeable in the beginning of the TSF Phase. Note that TSM-A1's algorithm to match GR-B in the  $e-\omega$  space to reduce the TSM-A2 magnitude violates the 10-km topographic altitude requirement for the  $-3\sigma$  case ( $\sim 7.5$  km—the red 10-km spherical altitude arc is crossed!). Also, although not shown in the plot,  $+3\sigma$  case violates the 10-km OPR COLA requirement ( $\sim 4$  km). The OPR COLA requirement will be examined more carefully in a later section.

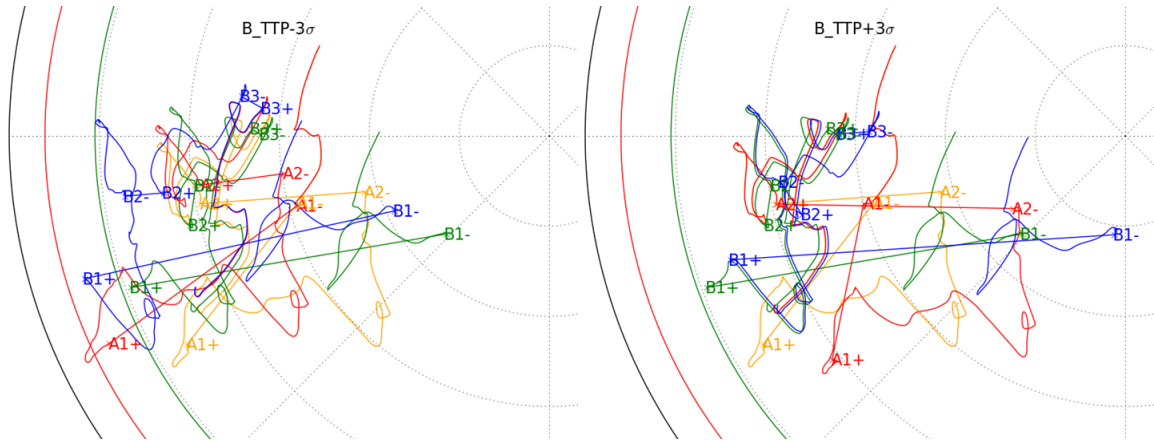


**Figure 14. GR-B  $\pm 3\sigma$  TTP Dispersion.**

Examining each of the 12 cases above against the derived requirements, we found only two items that were violated: (1) OPR COLA ( $\sim 4$  km  $<$  10 km) for the  $+3\sigma$  TTP dispersion case; (2) TSM-B1 topographic altitude constraint ( $\sim 7.5$  km). Thus, we can tentatively conclude that any  $\pm 3\sigma$  LOI delivery dispersions from TCM-B4 except for TTP are handled effectively by TSMs as long as GR-A dispersions remain near the nominal. Consequently, after analysis of both GR-A and GR-B dispersions individually, we concluded that the most critical LOI delivery parameters were TTP and RCA.

## ESTABLISHING TCM-5 GO/NO-GO CRITERIA

In this section we establish TCM-5 Go/No-Go criteria. However, the consideration of the COLA boundary is deferred to the next section due to its complexity.

### Boundaries for GR-A

We observed that any individual  $\pm 3\sigma$  GR-A dispersion from TCM-A4 is handled effectively by TSMs against the nominal GR-B. Here we attempt to show further that any  $\pm 3\sigma$  GR-A dispersion combinations can be handled effectively by TSMs against any  $\pm 3\sigma$  GR-B dispersion combinations other than TTP and RCA. For example, GR-A(+3 $\sigma$ , -3 $\sigma$ , +3 $\sigma$ , -3 $\sigma$ , +3 $\sigma$ , +3 $\sigma$ ) dispersion may be combined with GR-B(+3 $\sigma$ , 0, +3 $\sigma$ , -3 $\sigma$ , +3 $\sigma$ , 0) dispersion.\* Note that TTP and RCA dispersions remain zero or nominal for GR-B. There are  $2^6 = 64$  cases in total. All 64 runs were completed successfully.† The only problem was TSM-B3 magnitude being between 5.0 and 5.5 m/s in 8 cases. Since this problem can be fixed by placing TSM-B1 or TSM-A2 more intelligently by hand and 5.5 m/s is probably permissible, we just declare victory for the outcome. Since space does not permit us to show all 64  $e$ - $\omega$  plots, Figure 15 below shows only two example cases. The left one is GR-A(+3 $\sigma$ , -3 $\sigma$ , +3 $\sigma$ , -3 $\sigma$ , +3 $\sigma$ , +3 $\sigma$ ) + GR-B(-3 $\sigma$ , 0, -3 $\sigma$ , +3 $\sigma$ , -3 $\sigma$ , 0) as above. Although the GR-A dispersion is large coming into the TSF Phase, TSM-A1 and TSM-A2 handle it adequately while the TSM-Bs also handle the smaller GR-B dispersion adequately. The red and blue dispersed cases end up close together (appearing in purple) at the end of the TSF Phase, ready for science. The one on the right is just as easily handled by TSMs. Thus, we conclude that TSMs can handle any GR-A LOI delivery dispersions within  $\pm 3\sigma$  TCM-4 values as long as GR-B dispersions of TTP and RCA remain reasonable. When a case fails, it fails not due to GR-A dispersions (as long as they are within  $\pm 3\sigma$ ) but due to GR-B TTP and RCA dispersions. Thus, we focus our attention on TTP and RCA dispersions only from this point on, as they are indeed the two most critical parameters.

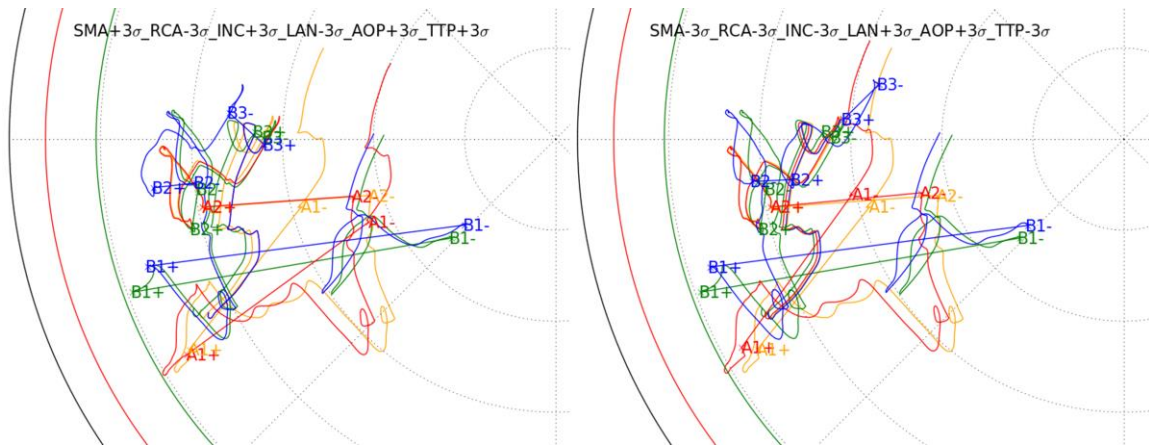


**Figure 15. Two Samples of  $\pm 3\sigma$  GR-A and  $\pm 3\sigma$  GR-B Dispersions (with 0 RCA & TTP).**

Now, Figure 16 below shows the TCM-A5 Go/No-Go boundary in the TTP vs. RCA axes with the  $\pm 3\sigma$  box and with 5,000 TCM-A4 and TCM-A5 LAMBIC samples overlaid in the background. The blue dots are 5,000 LAMBIC LOI delivery dispersion samples from TCM-A5

\* The same notation (SMA, RCA, INC, NOD, AOP, TTP) applies here as before.

† There were 32 cases of OPR COLA violation; however, the COLA problem will be dealt with in the next section.

projected onto the TTP vs. RCA axes; and the red dots are those from TCM-A4. The green x-marks are  $0, \pm\sigma, \pm2\sigma,$  and  $\pm3\sigma$  points from TSM-A4. There are 5,000 TCM-A5 samples (100%) and 4,985 TCM-A4 samples (99.7%) within the boundary. It predicts 99.7% chance of canceling TCM-A4 (not including COLA).

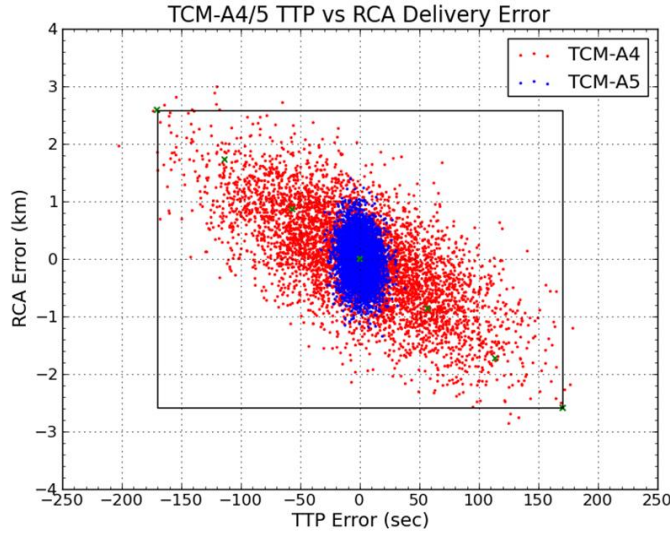


Figure 16. TCM-A5 Go/No-Go Boundary without COLA in TTP vs. RCA.

### Boundaries for GR-B

To establish the TCM-B5 Go/No-Go boundary, we start from a similar 5,000 LAMBIC samples for GR-B on TTP vs. RCA axes only. Note that we showed that the other GR-B parameters do not contribute significantly in determining the success or the failure of TSMs capability to handle the cases (without considering COLA).

*Left Bound.* For TCM-B5 Go/No-Go left boundary, we recall that the TCM-B1 topography altitude requirement is violated for a large negative TTP. A box is constructed to include some representative samples in the neighborhood of large negative TTP (Figure 17, left) and within the box an array of 11x8 points (with the TTP dispersions from -75 to -25 at a step of 5 seconds and the RCA dispersions from -1.5 to 3.0 at a step of 0.5 km). The run results are in terms of Pass/Fail (Green/Red) (Figure 17, middle). The minimum topographic altitude after TSM-B1 is shown in the contour plot (Figure 17, right). The black line is drawn along the 10-km altitude in the TTP vs. RCA axes. This line forms the left boundary for the TCM-B5 Go/No-Go criteria.

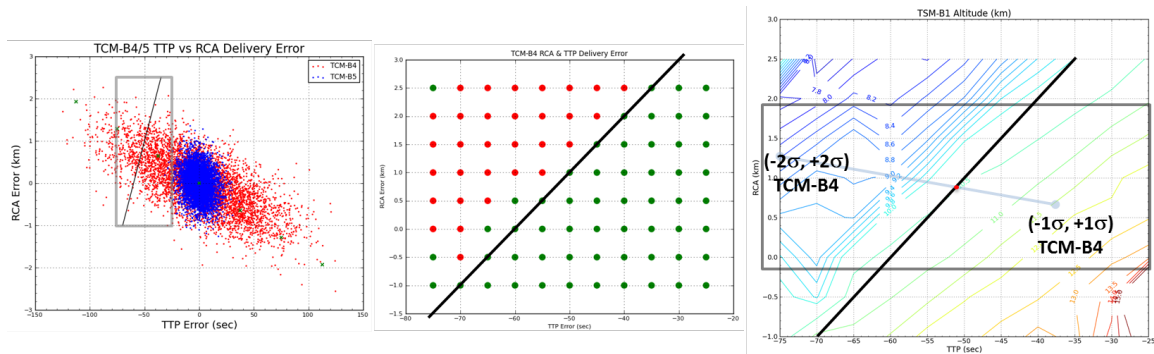
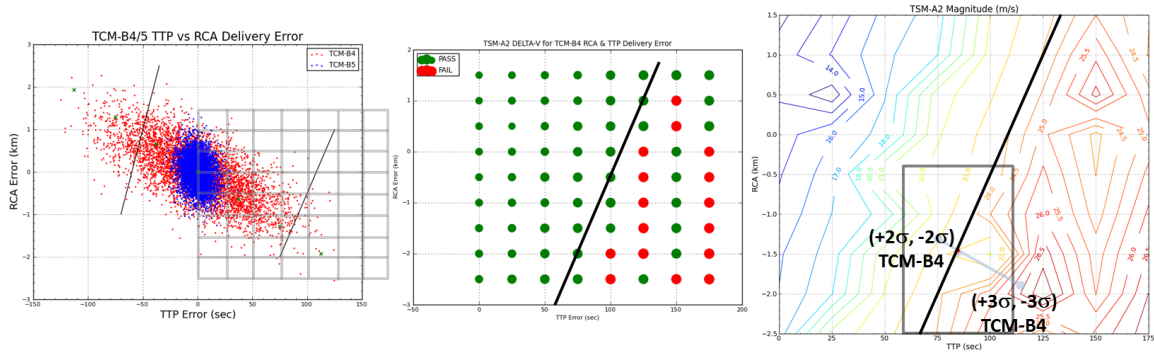


Figure 17. Left Bound for TCM-B5 Go/No-Go Boundary.

*Right Bound.* For the TCM-B5 Go/No-Go right boundary, it was observed that TSM-A2  $\Delta V$  magnitude increases slightly above the maximum requirement of 25 m/s for a large positive TTP. An array of 8x9 points are constructed with the TTP dispersions from 0 to 175 at a step of 25 seconds and the RCA dispersions from -2.5 to 1.5 at a step of 0.5 km. The run results are shown in Figure 18 below.\* The left plot shows the array. The middle plot shows pass/fail by color and  $\Delta V$  magnitude by the size of the circle and the right plot shows the contour map of the TSM-A2  $\Delta V$  magnitude. The black line marking 25 m/s maximum  $\Delta V$  is drawn in the TTP vs. RCA axes. This line forms the right boundary for the TCM-B5 Go/No-Go criteria.



**Figure 18. Right Bound for TCM-B5 Go/No-Go Boundary**

Thus, combining both the left and the right boundary and overlaying the TCM-B4 and TCM-B5 LAMBIC samples, Figure 19 below shows the TCM-B5 Go/No-Go boundary without COLA. The boundary includes 4,578 TCM-B4 samples (91.6%) and 5,000 TCM-B5 samples (100%). It predicts 91.6% chance of canceling TCM-B4 without considering COLA.

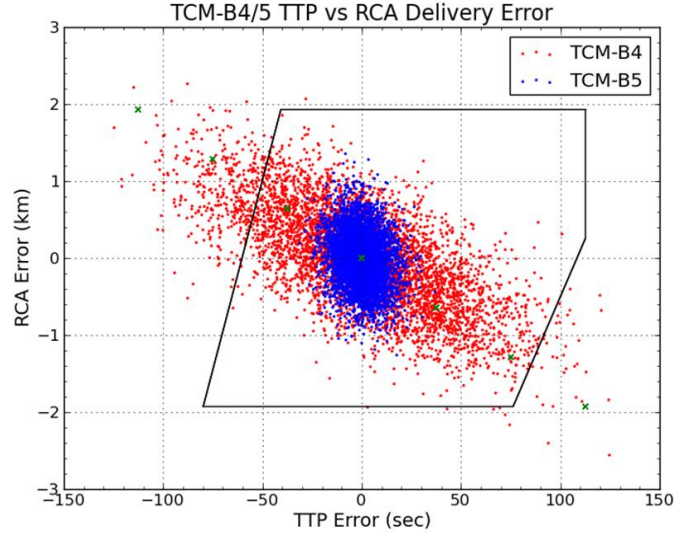


**Figure 19. TCM-B5 Go/No-Go Boundary without COLA in TTP vs. RCA.**

\* There were some COLA violations on these runs. We will use these results to simplify the COLA problem in the following section.

## ESTABLISHING COLA BOUNDARIES

COLA is inherently more complicated because GR-A and GR-B must be considered together unlike the previous boundaries where the effect of GR-A dispersion could be considered separate from that of GR-B dispersion. However, this does not apply to the COLA problem. So we must simplify the problem to be able to come up with some boundary helpful for operations.

### Some Simplification for COLA

We noted that there were some OPR violations while considering the 8x9 cases in determining the GR-B right bound. This COLA result is summarized on the left plot of Figure 20 below. The green circle represents separation above 10 km. The red represents COLA between 0 and 10 km. The magenta denotes a negative number, which represents an orbit crossing. Note also that the 10-km COLA boundary line has a slope of 4 km / 25 second (the blue line). Now, to reduce the number of cases to compute and visualize, we assume that all the points on a line with this slope in TTP vs. RCA space have the same COLA values. Under this simplification we can transform TTP and RCA parameters (2 dimensions) into one parameter (1 dimension), which we shall call “effective sigma.” The effective sigma lies on a line with a slope of -1 where  $\sigma(\text{RCA}) = -\sigma(\text{TTP})$ . To transform TTP and RCA to an effective sigma, we first convert the TTP and RCA dispersions into its corresponding sigma:  $\sigma(\text{TTP})$  and  $\sigma(\text{RCA})$ . The effective sigma,  $\sigma(\text{effective})$ , can then be computed as follows:

$$\sigma(\text{effective}) = (m * \sigma(\text{TTP}) - \sigma(\text{RCA})) / (m + 1)^*$$

where  $m_A = 10.530$  for GR-A (from the COLA line slope, 4 km / 25 sec, for GR-A  $\sigma$  values) and  $m_B = 9.342$  for GR-B (from the same slope for GR-B  $\sigma$ ). In this way the two dimensions of (TTP, RCA) are reduced to only one  $\sigma(\text{effective})$ , allowing a COLA contour plot of GR-A  $\sigma(\text{effective})$  vs. GR-B  $\sigma(\text{effective})$  to be generated relatively with ease and visualized. Figure 20 shows the contour plot of the minimum COLA in terms of GR-B  $\sigma(\text{effective})$  vs. GR-A  $\sigma(\text{effective})$ .

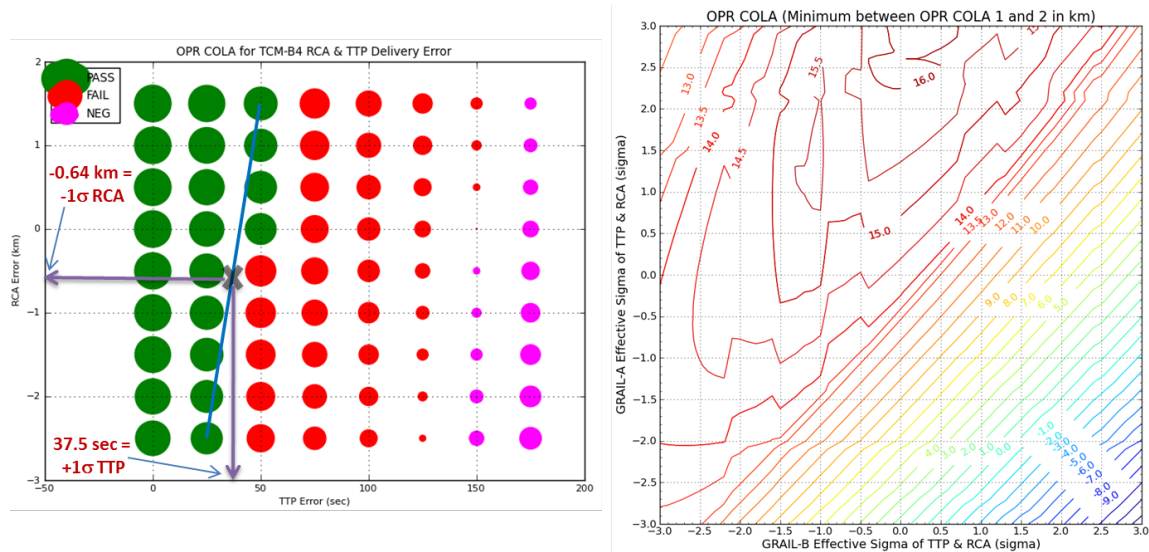


**Figure 20. Minimum COLA between OPR COLA and TSF COLA.**

\* This formula was obtained simply from the intersection of  $Y = -X$  (the effective  $\sigma$  line) and  $Y = m * X + b$  (the OPR COLA line from Figure 20) where  $m$  is the slope of the OPR COLA line, empirically found to be 4 km / 25 seconds.

## COLA Boundaries for GR-A and GR-B

From the contour plot in Figure 20 above, GR-A  $\sigma(\text{effective})$  depends on the selection of the GR-B  $\sigma(\text{effective})$  for a given COLA distance. Note that if a high positive value were selected for GR-B  $\sigma(\text{effective})$  to have a larger GR-B No-Go boundary, it translates to a high GR-A  $\sigma(\text{effective})$  according to the contour plot. Thus, it would be difficult to have an equally large GR-A No-Go boundary at the same time. To have a larger GR-A No-Go boundary, GR-B  $\sigma(\text{effective})$  must be as low as possible. In other words, the GR-B OPR boundary is intimately related with the GR-A OPR boundary. We must reach a happy medium.\*

*GR-B COLA Bound.* We decided on the GR-B COLA boundary that barely encompasses  $\pm 3\sigma$  TCM-B5 TTP & RCA dispersions since anything below this would have required the execution of TCM-B5. Figure 21 below shows a proposed GR-B COLA bound on the left. The  $\pm 3\sigma$  TCM-B5 dispersion box is shown in green. The  $\sigma(\text{effective})$  line is in brown. The cyan line is the proposed line for GR-B COLA bound that just barely touches the green box. This cyan line crosses the brown  $\sigma(\text{effective})$  line at  $0.8 \sigma(\text{effective})$ , which translates to  $+0.8 \sigma(\text{TTP})$  and  $-0.8 \sigma(\text{RCA})$ . Out of 5,000 LAMBIC samples, this bound includes 71.5% of the TCM-B4 samples and 99.96% of the TCM-B5 samples. It predicts 71.5% chance of canceling TCM-B4 including COLA.

*GR-A COLA Bound.* Now, to determine the GR-A COLA boundary for the given GR-B COLA boundary of  $0.8 \sigma(\text{effective})$ , we look for a possible GR-A  $\sigma(\text{effective})$  at  $0.8 \sigma(\text{effective})$  GR-B from the contour plot in Figure 20 above. A few considerations are: (1)  $-0.4\sigma(\text{effective})$  for 10 km COLA (the green line in Figure 21 right, which corresponds to 68.5% without and 99.6% with TCM-A5); (2)  $-1\sigma(\text{effective})$  for 7.5 km COLA (the cyan line in Figure 21 right, which corresponds to 85% without and 100% with TCM-A5); (3)  $-2\sigma(\text{effective})$  for 3 km COLA (the magenta line in Figure 21 right, which corresponds to 98% without and 100% with TCM-A5). We chose option 2. This line at  $-1 \sigma(\text{effective})$  is shown in cyan on the right plot in Figure 21 below.

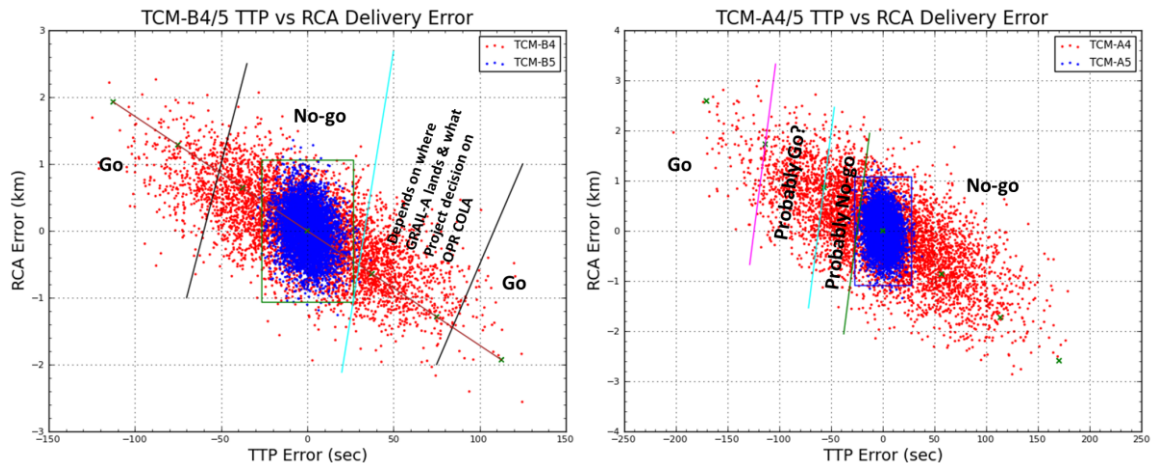
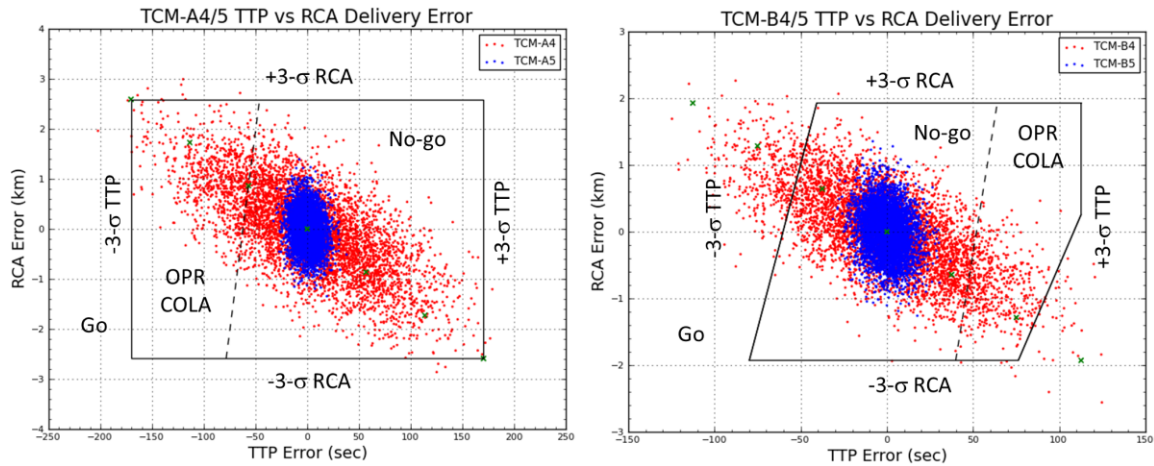


Figure 21. Proposed GR-B & GR-A COLA Bounds.

\* However, as soon as GR-A TTP & RCA dispersions are actually known after TSM-A4, we would be able to determine the actual GR-A  $\sigma(\text{effective})$  and to fix the GR-B  $\sigma(\text{effective})$  from the OPR contour in Figure 20, given the COLA distance.

## FINAL TCM-5 GO/NO-GO BOUNDARIES

Combining all the results so far, we have the following final TCM-5 Go/No-Go boundaries including COLA boundaries in Figure 22 below.



**Figure 22. Final TCM-5 Go/No-Go Boundaries.**

## CONCLUSION

Both TCM-4s had to be executed since they were well outside of the boundaries as expected. As it turned out, TCM-A4 hit the maximum cut-off timer, so was slightly low on the magnitude; nevertheless, GR-A was found well within the TCM-A5 No-Go boundary. TCM-A5 was canceled. The maximum cut-off timer on GR-B was increased by 20% to avoid the issue. GR-B also landed within the boundary. TCM-B5 was also canceled. Refer to Figure 23 below for the orbit determination (OD) solutions and their associated uncertainty error ellipses within the boundaries. Note that the OD uncertainty ellipse shrinks in size as the spacecraft approaches the Moon.

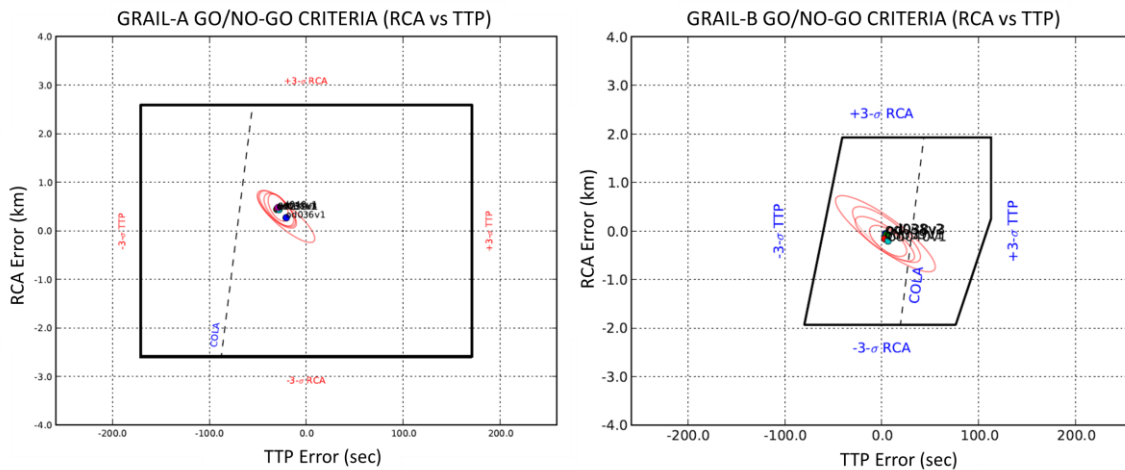


**Figure 23. The ODs and Uncertainty Ellipses near the time of TCM-A5 and TCM-B5.\***

\* These plots with ODs and their shrinking uncertainty ellipses were generated by Brian Young (Maneuver Analyst, JPL).

## ACKNOWLEDGMENTS

This work was performed at the Jet Propulsion Laboratory (JPL), California Institute of Technology, Pasadena, California under contract to National Aeronautics and Space Administration. The author wishes to thank Ralph B. Roncoli and Roby S. Wilson of JPL for their review of the paper. The author also wishes to thank all the GRAIL navigation team members, including: Peter Antreasian, Ram Bhat, Kevin Criddle, Sara Hatch, Troy Goodson, David Jefferson, Julie Kangas, Eunice Lau, Ralph Roncoli, Mark Ryne, Ted Sweetser, Tung-Han You, Brian Young, Hui Ying Wen, Mau Wong for their support and for the successful navigation of the mission.

## REFERENCES

- <sup>1</sup> Roncoli, R. B., and Fujii, K. K., Mission Design Overview for the Gravity Recovery and Interior Laboratory (GRAIL) Mission, AIAA/AAS Astrodynamics Specialist Conference, 2010 AIAA Meeting Papers on Disc, Vol. 15, No. 9 (GNC/AFM/MST/Astro/ASE), AIAA, Washington, DC, 2010.
- <sup>2</sup> Chung, M. J., Hatch, S. J., Kangas, J. A., Long, S. M., Roncoli, R. B., and Sweetser, T. H. Trans-Lunar Cruise Trajectory Design of GRAIL (Gravity Recovery and Interior Laboratory) Mission, AIAA/AAS Astrodynamics Specialist Conference, 2010 AIAA Meeting Papers on Disc, Vol. 15, No. 9 (GNC/AFM/MST/Astro/ASE), AIAA, Washington, DC, 2010.
- <sup>3</sup> Hatch, S. J., Roncoli, R. B., and Sweetser, T. H. GRAIL Trajectory Design: Lunar Orbit Insertion through Science, AIAA/AAS Astrodynamics Specialist Conference, 2010 AIAA Meeting Papers on Disc, Vol. 15, No. 9 (GNC/AFM/MST/Astro/ASE), AIAA, Washington, DC, 2010.
- <sup>4</sup> E. H. Maize, "Linear Statistical Analysis of Maneuver Optimization Strategies," *AAS/AIAA Astrodynamics Specialist Conference*, Kalispell, Montana, AAS 87-486 (August 1987).
- <sup>5</sup> Sweetser, T. H., How to Maneuver Around in Eccentricity Vector Space, AIAA/AAS Astrodynamics Specialist Conference, 2010 AIAA Meeting Papers on Disc, Vol. 15, No. 9 (GNC/AFM/MST/Astro/ASE), AIAA, Washington, DC, 2010.